Journal of Sound and Vibration (1999) **220**(2), 203–224
Article No. jsvi.1998.1938, available online at http://www.idealibrary.com on IDEAL

STRUCTURE-BORNE SOUND POWER AND SOURCE CHARACTERIZATION IN MULTI-POINT-CONNECTED SYSTEMS, PART 2: ABOUT MOBILITY FUNCTIONS AND FREE VELOCITIES

R. A. FULFORD† AND B. M. GIBBS
Acoustics Research Unit, University of Liverpool, L69 3BX, England

(*Received* 26 *March* 1997, *and in final form* 27 *July* 1998)

As an aid to the control of structure-borne sound the characterization of a machine as a structure-borne sound source would constitute a useful design tool. Towards this goal, a formulation based upon a machine's ability to deliver power has been proposed by Mondot and Petersson [1]. To progress their proposal, this paper examines in an ordered manner those physical parameters which determine the vibrational power in a system involving multiple connections. The structural characteristics of typical machine and floor mount conditions are considered by examination of mobility relationships whilst the machine excitation (or source activity) characteristics are considered via free velocity relationships.
© 1999 Academic Press

1. INTRODUCTION

When a machine (the source) is connected to a supporting structure (the receiver) the structural coupling is such that in general the resultant dynamic behaviour of the combined system is dependant upon both the source and receiver structural characteristics and the excitation of the source (its activity). That the system behaviour is dependent upon both bodies means henceforth that it is difficult to relate the behaviour of the combined system to source-only parameters. Clearly the characterization of a machine as a vibrational source is therefore inherently problematic.

In an attempt to circumvent the problem, Mondot and Petersson [1] proposed that source characterization be considered with respect to the ability of a machine to deliver vibrational power. For each connection point and degree of freedom two functions are introduced; the source descriptor,

$$S_i^n = (V_{sf_i}^n)^2 / 2\, Y_{s_{ii}}^{nn\Sigma *}, \tag{1}$$

and the coupling function,

$$Cf_i^n = Y_{s_{ii}}^{nn\Sigma *}\, Y_{r_{ii}}^{nn\Sigma *} / |\, Y_{s_{ii}}^{nn\Sigma} + Y_{r_{ii}}^{nn\Sigma}\,|^2, \tag{2}$$

† Institut für Technische Akustik, T-Universität, 10587 Berlin, Germany

0022–460X/99/070203 + 22 $30.00/0 © 1999 Academic Press

where $V^n_{sf_i}$ is free velocity, $Y^{nn\Sigma}_{s_{ii}}$, $Y^{nn\Sigma}_{r_{ii}}$ are effective point mobilities [2] of the source and receiver respectively and n denotes position and i component direction.

Physically the source descriptor can be considered as describing the ability of the source to produce power and the coupling function thought of as a filter determining how much of this latent power is manifested is the combined system. The manifested power is obtained via their product and the total power in the combined system is obtained by summation of such over all connection points and components of direction.

Whilst the approach has clear promise [3] a key difficulty inherent is that it relies upon formulation of the effective point mobilities;

$$Y^{nn\Sigma}_{ii} = Y^{nn}_{ii} + \sum_{m=1,m\neq n}^{N} Y^{nn}_{ii}\frac{F^m_i}{F^n_i} + \sum_{j=1,j\neq i}^{6} Y^{nn}_{ij}\frac{F^n_j}{F^n_i} + \sum_{m=1,m\neq n}^{N}\sum_{j=1,j\neq i}^{6} Y^{nm}_{ij}\frac{F^m_j}{F^n_i}, \qquad (3)$$

where Y^{nm}_{ij} is mobility and F^m_i force.

As well as the force distribution amongst the contact points, formulation of all the effective point mobilities does therefore require knowledge of all the source and receiver mobilities of the system. Even with reciprocity invoked, the amount of data is demanding; i.e., for a four contact system with six degrees of freedom 300 separate mobility spectra, for both source and receiver, are required. Moreover, whilst it is clear that such an amount of data can seldom be procured reliably, the problem is compounded upon understanding that the force distribution in the system is, together with all the source and all the receiver mobilities, also dependant upon the free velocities of the source. To calculate the source descriptor prior to assemblage of the system, all such parameters therefore either need to be measured, predicted or estimated in some manner.

Henceforth, and as discussed in an earlier paper by Fulford and Gibbs [2], it is suggested that, in regard to the source descriptor and coupling function formulation there is much to be gained by considering it with a view to understanding, and possibly generalizing their forms, the mobilities of machines and supporting structures together with the machine free velocities. Also, if relationships amongst the terms can be found the amount of data needed to be procured before formulation of the effective point mobilities, and following the source descriptors and coupling functions, can be reduced. For example, upon assuming only translational motion, equation (3) can be rewritten as

$$Y^{nn\Sigma} = \sum_{m=1,m\neq n}^{N} Y^{nn}\left(\frac{Y^{mn}}{Y^{nn}}\right)\frac{F^m}{F^n}, \qquad (4)$$

to reveal that if Y^{mn}/Y^{nn} (the ratio of transfer to point mobility) can be assumed then knowledge of the individual transfer mobilities is not required.

Hence with the purpose of understanding and appreciating their forms, this paper investigates mobilities and free velocities for typical mount conditions. Whilst it is recognized that all components of motion at each contact should be studied, the work is limited to the important case of vertical translational motion and to four contact points. Further, from understanding that even small structural

changes can influence a mobility [4]; an engineering approach is adopted in that the work is directed towards a generic form of result.

2. MACHINE MOBILITIES

For a large range of machines, the mount footing is typically a plate [5]. With this assumption the dynamics of a mount can be modelled as a plate attached via a spring to a mass (see Figure 1) where the mass represents the machine body and the spring the local stiffness of the footing as determined by the boundary conditions, material and dimensions of the plate. By using this model, the point mobility, prior to the onset of wave behaviour within the plate, can be expressed as

$$Y = (k - \omega^2 M)/\mathrm{i}\omega M k, \tag{5}$$

where M is the mass of the machine and k the local stiffness of the mount footing.

For low frequencies the mass term will dominate the expression so that the mobility will exhibit a mass controlled region (magnitude decrease of 6 dB per octave with a phase of $-\pi/2$) whilst for high frequencies the stiffness term will dominate to give a stiffness controlled region (magnitude decrease of 6 dB per octave with a phase of $\pi/2$). Where the mass and stiffness behaviour counteract each other, and therefore separating these two regions, will be an anti-resonance frequency

$$\omega_o = \sqrt{K/m}. \tag{6}$$

For frequencies beyond the stiffness controlled region, the plate will begin to bend and at its fundamental frequency there will be an onset of resonant behaviour whereupon in regard to the mobility the specifics of the plate (and then the machine body) become important and any analysis would require a detailed model.

With respect to the forms of the mobilities, it is useful therefore to understand that the point mobility of a typical machine mount will exhibit in general all of mass, stiffness and resonant controlled regions, and that the mass and stiffness regions are separated by a anti-resonance determined by the mass and local stiffness, whilst the onset of the resonant region is determined by the properties of the mount plate. Upon assuming therefore a generalized form of the point

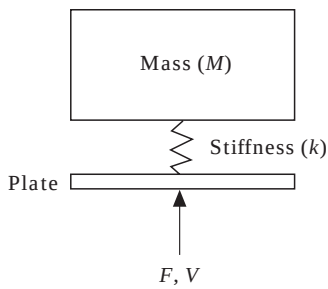

Figure 1. Model of a machine mount point.

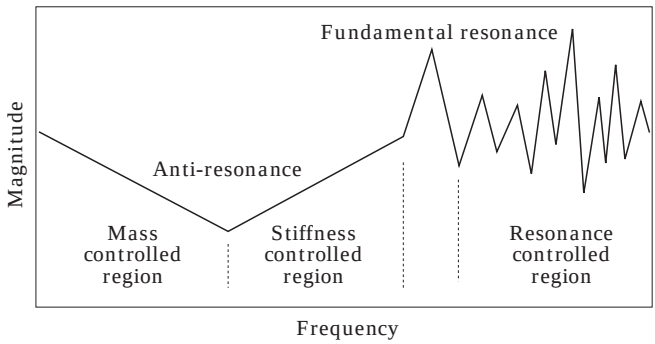

Figure 2. Generalized point mobility of machine mount.

mobility as shown in Figure 2, it is orderly to consider the relationships between the point and transfer mobilities in each region separately.

2.1. MASS CONTROLLED REGION

In the mass controlled region the machine can be modelled as a rigid body and, upon assuming that the co-ordinate axes coincide with the principal inertia axes of the body, the mobility can be given by

$$Y = (1/\mathrm{i}\omega)(1/m + y_o y/I_{xx} + x_o x/I_{yy}), \tag{7}$$

where x_o and y_o describe the position of the force with respect to the centre of gravity, x and y are the co-ordinates of the response point and, I_{xx} and I_{yy} are the moments of inertia.

The expression reveals that in the mass controlled region, the point and transfer mobilities are dependent upon the position of the points involved and upon the machine's moments of inertia. Relationships for the point and transfer mobilities can therefore only be procured if values for such are introduced. Towards this, it is suggested that two basic types of machines can be considered; one in which both the $y_o y/I_{xx}$ and $x_o x/I_{yy}$ terms of equation (7) are small compared to the $1/m$ term, i.e., the machine is "tall", and one in which all of the terms are comparable, i.e., the machine is "squat".

For the former, the simple relationship deduced is that the transfer mobility, Y^{tr}, will approximate to the point mobility, Y^{pt}: i.e., Y^{tr}/Y^{pt} is approximately unity. To deduce relationships for the latter type it is suggested that for practical reasons of stability many machines are designed such that the centre of gravity is near the geometrical centre and that the mount points are positioned symmetrically around this point. With reference to Figure 3, the following then applies for the magnitude of the point mobilities,

$$Y^{11} \approx Y^{22} \approx Y^{33} \approx Y^{44}, \tag{8a}$$

and for the transfer mobilities,

$$Y^{12} \approx Y^{34}, \qquad Y^{13} \approx Y^{24}, \qquad Y^{14} \approx Y^{23}. \tag{8b–d}$$

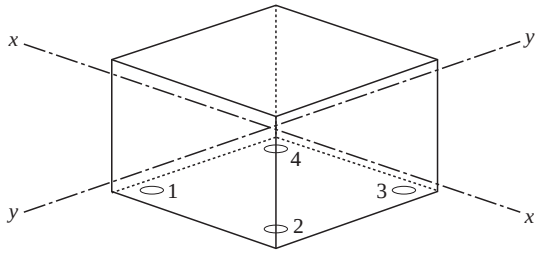

Figure 3. Machine with a plate-like base.

By definition, the phase of the point mobilities is always $-\pi/2$ in the mass controlled region whilst the phase of the transfer mobilities depends upon I_{xx} and I_{yy} and the positions of the mount points. Upon assuming again that the positions are symmetric about the centre of gravity, two conditions are likely, one where I_{yy} is greater than I_{xx} and one where I_{xx} is greater than I_{yy} (the case where I_{xx} and I_{yy} are equal and small is theoretically possible but unlikely in practice). For the first case,

$$\theta\{Y^{12}\} = \theta\{Y^{11}\} = -\pi/2, \qquad \theta\{Y^{13}\} = \theta\{Y^{14}\} = \pi/2, \tag{9a, b}$$

and for the second case,

$$\theta\{Y^{14}\} = \theta\{Y^{11}\} = -\pi/2, \qquad \theta\{Y^{12}\} = \theta\{Y^{13}\} = \pi/2. \tag{10a, b}$$

Unless the details of the machine are known, the above it is suggested, represents all which can be deduced as regards the mobility relationships of a machine in a mass controlled region.

2.2. STIFFNESS CONTROLLED REGION

In the stiffness controlled region, the mobility is primarily controlled by the structural characteristics of the mount plate, i.e., size, material and boundary conditions, and the main body of the machine can be ignored in the analysis. Upon assuming thin-plate theory [6] the forced transverse motion of the mount point is governed by

$$D[\partial^4 W/\partial x^4 + 2\,\partial^4 W/\partial^2 x\,\partial^2 y + \partial^4 W/\partial y^4] + \rho h\,\partial^2 W/\partial t^2 = F(x, y)f(t), \tag{11}$$

where x, y, z are the mutually perpendicular co-ordinates, t is the time function, W is transverse displacement, ρ is density, h the plate thickness and F the applied force. D is the flexural rigidity of the plate and is given by

$$D = Eh^3/12(1 - v^2), \tag{12}$$

where v is the Poisson's ratio of the material and E the Young's modulus. Unless at least one pair of opposite edges are simply supported, solution is possible only by approximate methods. Of these, the Rayleigh–Ritz approach [7] is most versatile as regards boundary conditions and was adopted for the study.

The analysis makes a distinction between the mount condition being either plate- or flange-like. With a plate-like base (see Figure 3) all mount points are upon a single homogeneous plate whilst for a flange-like base (see Figure 4) not only

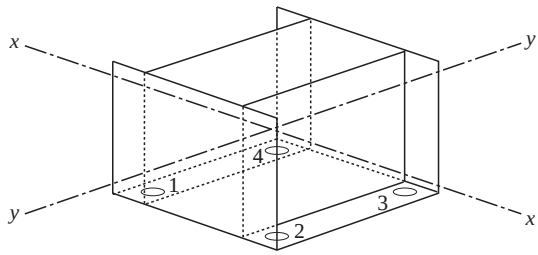

Figure 4. Machine with a flange-like base.

can discontinuities exist between mount points but moreover its characteristic is that one dimension is much greater than the other and at least one long side has a free-edge condition. The mobilities are considered for each base type in turn.

2.2.1. *Plate-like base*

If the machine has a box-like construction where the thickness of the base is greater than that of the supporting walls, the plate can be characterized as being simply supported along all four edges: i.e., a SSSS plate. For such, if two points are both far from an edge the difference between point and transfer mobilities in the stiffness controlled region will be small (see Figure 5, where a $1\text{ m} \times 1\text{ m} \times 5\text{ mm}$ steel plate has been assumed) and Y^{tr}/Y^{pt} will tend to unity. If one point is close to an edge however the constraint imposed upon the deflection is such that significant differences between the two mobilities can occur (see Figure 6). Since the deflection is not uniform over the plate area, differences can also occur if the two points are a significant distance apart. Although the positions of, and distance between, the mount points cannot be assumed, for practical purposes the mounts can (likewise for the mass controlled region) be assumed symmetrically positioned around the geometric centre. Doing so allows the transfer mobilities in the stiffness region to be paired as in equation (8).

Where the supporting edge thickness is equal to, or greater than, that of the base-plate the boundary conditions are approximated by a clamped condition. Although for such it is known that the stiffness differs greatly at positions close to the edge cf. at the centre, Y^{tr}/Y^{pt} can be assumed unity providing both points

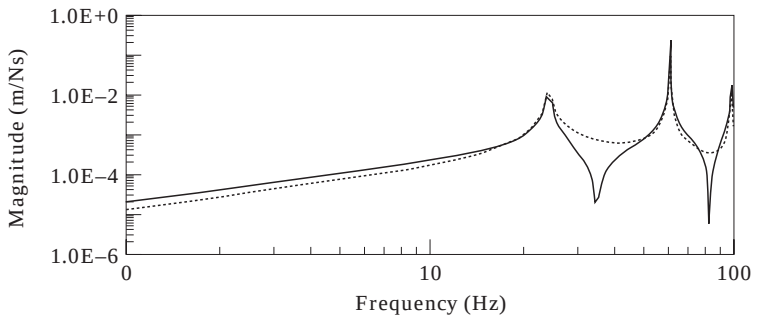

Figure 5. Typical point and transfer mobilities for non-edge positions on a SSSS plate. —, Y^{pt}; . . . . , Y^{tr}.

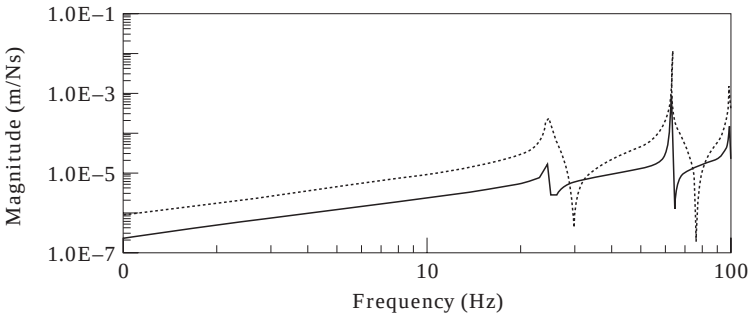

Figure 6. Typical point and transfer mobilities of a SSSS plate where one point is close to an edge. Key as Figure 5.

are away from an edge. A paired condition, equation (8), can then again be imposed if a symmetrical configuration is assumed.

In the region, the phase of the point mobilities will, by definition, be $\pi/2$. Also, since there is no global movement of the body in the phase of the transfer mobilities will likewise be $\pi/2$.

2.2.2. *Flange-like base*

One example of a flange-like base is the cantilever with three free edges (see Figure 7). Upon assuming a clamped fixed edge and an aspect ratio of 10, point

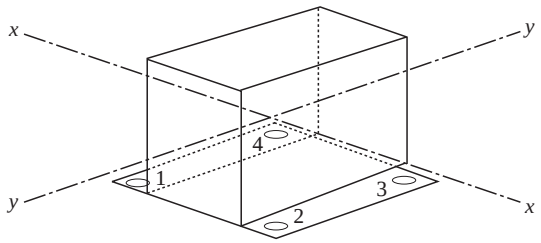

Figure 7. Machine with cantilever flanges.

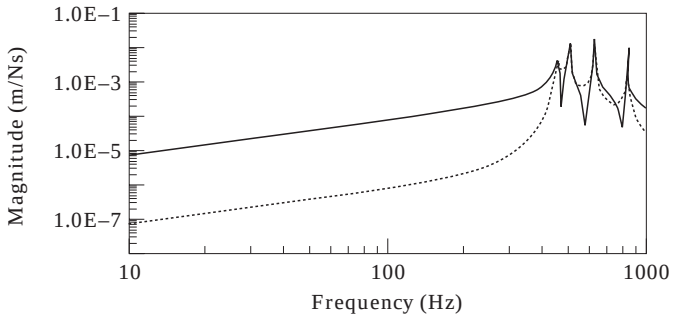

Figure 8. Typical point and transfer mobilities for a CFFF flange. Key as Figure 5.

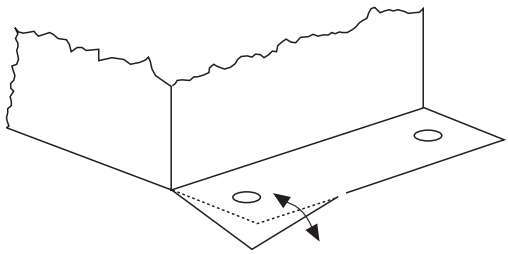

Figure 9. Local plate deformation.

and transfer mobilities are as shown in Figure 8 for typical mount positions on a 5 mm thick steel flange. It is seen that in the stiffness controlled region (in this case, up to 400 Hz), the transfer mobility is less than that of the point mobility but converges rapidly to it at the fundamental frequency. Such behaviour occurs because in the stiffness region the plate is twisting with localized deformation (see Figure 9) whilst at resonance the deformation is global and the whole plate is excited. Though the details of this behaviour are dependent upon all of the material, aspect ratio and thickness of the flange, the analysis can be rationalized to an extent by assuming the ratio of the transfer to point mobility in the stiffness controlled region has a frequency invariant form: i.e.,

$$Y^{tr}/Y^{pt} = Yk^{pt}/Yk^{tr}, \tag{13}$$

where Yk^{pt} represents the point mobility stiffness and Yk^{tr} the transfer mobility stiffness. Then, for typical materials and flange thickness Y^{tr}/Y^{pt} can be expressed as a function of aspect ratio. Hence, upon assuming the flange material to be steel and its thickness to be 5 mm, Figure 10 is produced. Two regions either side of a minimum at $b/a = 7$ are seen, the first where Yk^{tr}/Yk^{pt} decreases as b/a is increased and the second where it increases.

It is proposed that the transfer stiffness has two components Y^{ktr}_{defl} and Y^{ktr}_{bend}. Due to the twisting action of the plate the two mount points will have different deflections relative to the clamped edge, and therefore an associated difference in stiffness, this being accounted for by the component Y^{ktr}_{defl}. Differences in stiffness

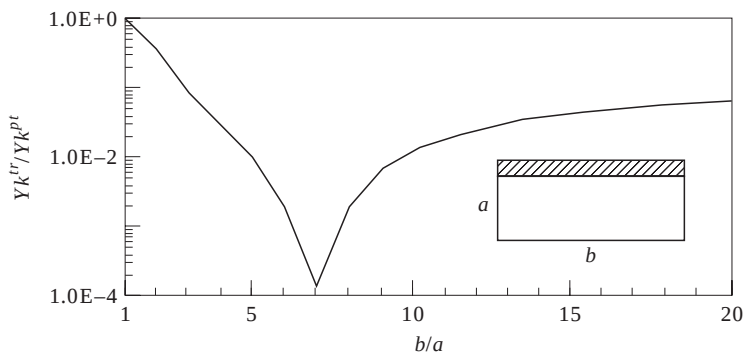

Figure 10. Typical Yk^{tr}/Yk^{pt} for a CFFF flange.

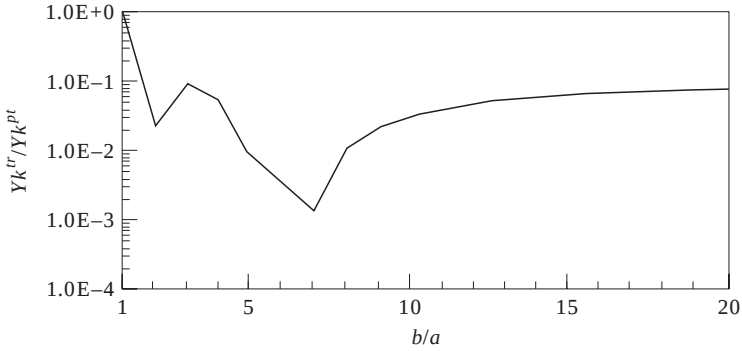

Figure 11. Typical Yk^{tr}/Yk^{pt} for a CFCF flange.

also occur due to the curvature of the plate along the line between the two points and this is accounted for by Y^{ktr}_{bend}.

Since Y^{ktr}_{bend} is associated with a bending mode, it is dominant where Yk^{tr}/Yk^{pt} is curved i.e., $b/a < 7$, whilst Y^{ktr}_{deft} is dominant for $b/a < 7$. The aspect ratio at which the two regions converge (7) can be expected to alter for flanges of differing thickness and material. As such its value is of limited significance.

If the position of the excitation point is moved towards the clamped edge, the twisting action of the plate will reduce and the transfer mobility compared to the point mobility can be expected to decrease. Conversely if the excitation point is moved towards the free edge, the twisting action will be greater and the transfer mobility compared to the point mobility can be expected to increase.

Whilst Yk^{tr}/Yk^{pt} is dependent upon all of aspect ratio, material, plate-thickness and the position of the mount points it is suggested that typically Y^{tr} along a clamped cantilevered plate can, for a stiffness controlled region, be considered to be an order of magnitude or more, less than Y^{pt}. Other flange-like bases include the cases where two opposite sides are fixed or where three sides are fixed. Since the boundary conditions of a real fixed edge are known to be between the simply supported and clamped conditions [8] both are considered. For typical excitation and reception points, Yk^{tr}/Yk^{pt} is shown in Figure 11 for a CFCF 5 mm steel plate and in Figure 12 for a SFSF 5 mm steel plate. Again two regions are seen and

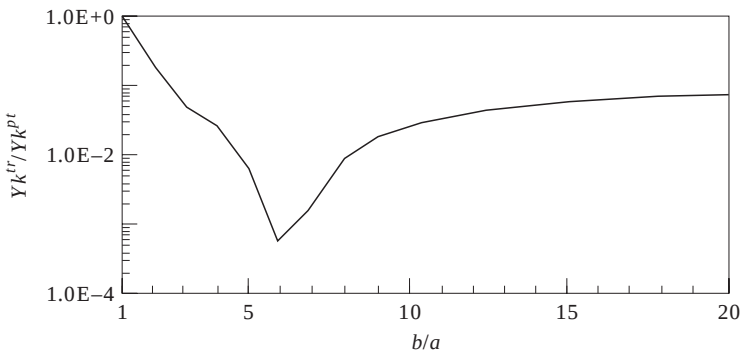

Figure 12. Typical Yk^{tr}/Yk^{pt} for a SFSF flange.

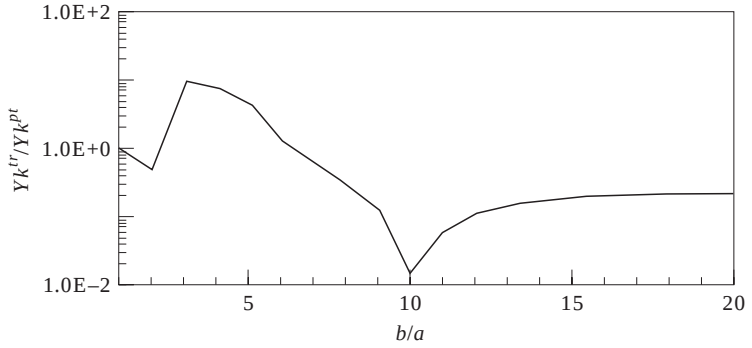

Figure 13. Typical Yk^{tr}/Yk^{pt} for a CCFC flange.

again the magnitude of the transfer mobility tends to be at least a decade below that of the point mobility.

Where the plate is CCFC, Yk^{tr}/Yk^{pt} is shown in Figure 13 and where it is SSFS in Figure 14. For the latter, the ratio is invariant with respect to b/a for $b/a > 6$ but the magnitude of the transfer mobility is again approximately a fifth of the point mobility. For the CCFC plate however Yk^{tr} is a decade less that Yk^{pt} for $b/a > 8$. Further, for $2 < b/a < 6$, Yk^{tr} is greater than Yk^{pt}. Whilst the CCFC case does not permit general conclusions, the ratio Yk^{tr}/Yk^{pt} for a plate fixed on three sides can again clearly be small; i.e., 10^{-1}.

Henceforth, it is suggested that for any flange the general trend is for the transfer mobility to be approximately a decade below that of the point mobility. If it is also assumed that the flanges are attached to the machine through strong discontinuities, the relationship amongst the mobilities in the stiffness controlled region needs to take into account only the number of flanges involved and their configuration, i.e., for two points across a strong discontinuity

$$Y^{tr} = 0, \tag{14}$$

whilst for two points along a flange

$$Y^{12} \approx Y^{11}/10. \tag{15}$$

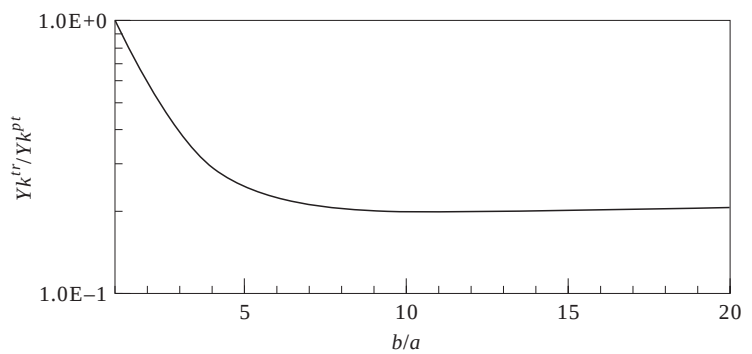

Figure 14. Typical Yk^{tr}/Yk^{pt} for a SSFS flange.

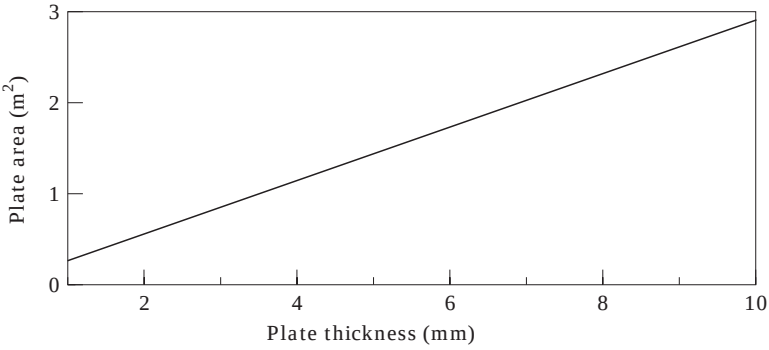

Figure 15. For steel and $\eta = 0{\cdot}001$, area of plate necessary for Skudrzyk's high frequency limit.

2.3. RESONANCE CONTROLLED REGION

In the resonance region, the transfer and point mobility are dependent upon the modal interaction of the machine base; be it flange- or plate-like. Since the mode shapes and mode frequencies are dependent upon the material, dimensions and boundary conditions and the modal interaction is dependent upon the frequency, excitation position, reception position and material damping, the establishment in the resonance region of Y^{tr}/Y^{pt} relationships is difficult. This was highlighted in a seminal paper by Skudrzyk [9].

In his paper Skudrzyk subdivided the resonance region into four frequency ranges: (i) low frequencies; (ii) transition frequencies; (iii) high frequencies and (iv) very high frequencies with the ranges determined by the ratio of average modal spacing to the half-power bandwidth of a mode,

$$\alpha = \epsilon_v/\eta\omega_v, \tag{16}$$

where ϵ_v represents the average modal spacing (rad/s), η the material loss factor and ω_v the frequency of interest.

For regions (iii) and (iv) α is defined as approximate to or less than unity respectively. As regards the mobilities of machines, it can however be argued that these frequencies are not of concern. To illustrate, the modal spacing for a thin mount plate transversely excited is deduced from reference [13] to be

$$\epsilon_v = 3{\cdot}6c_L h/A, \tag{17}$$

where A is the plate area and c_L is the quasi-longitudinal wave propagation speed. Then, equations (16) and (17) combined give

$$\alpha = 3{\cdot}6c_L h/\eta A\omega_v, \tag{18}$$

whereupon, for the assumed material properties of steel, a loss factor of 0·001 and an upper frequency limit of 10 kHz, the plate area required for α to equal unity is shown in Figure 15 as a function of plate thickness. Henceforth, for plate thicknesses of 3 mm or less, it is seen that a plate area of 1 m^2 or less can accommodate α equal to unity whilst for thicker plate thicknesses the area necessary is larger than 1 m^2. It is suggested that "typically" the mount plates of building engineering machines are "thick" whereby for an $\alpha = 1$ condition to exist

the plate area needed is 1 m^2. Such an area is thought to be above that usually encountered and in the following it is inferred that for machine mobilities the high and very high frequency regions of Skudrzyk are not applicable.

For Skudryzk's transition range, α is between unity and five. For a steel plate of thickness of 3 mm and, once more, an upper frquency of 10 kHz, the range of plate areas to which these limits correspond has a lower bound of about 0·2 m^2. This area is suggested to be of practical concern. Whilst therefore it would be useful to obtain simple Y^{tr}/Y^{pt} relationships for this range, Skudrzyk has concluded that no simple general theory to describe a mobility can be expected. The reasoning is that the range describes the transition from "many" to "few" reflections contributing to the wavefield and, as neither a statistical nor smoothed description of the mobility functions is applicable, Y^{tr}/Y^{pt} has to be determined uniquely for any given case.

Of most interest therefore is Skudrzyk's work in the low frequency region where $\alpha > 5$, an engineering description for this range being where the mobility has well separated peaks. Even for this region it should be acknowledged however that for all but very simple structures it is not possible to predict exact mobility spectra. Hence at most, only the mean of the mobility magnitude and the envelope which bounds the upper and lower peaks can be predicted with any reliability. As such only a statistical distribution involving the mean and range of Y^{tr}/Y^{pt} is considered.

As regards the mean of a point mobility, if the point is at the centre of a plate this will be equal to the characteristic plate mobility. Where the point is within a wavelength of a free edge an increase above this value of about 5 dB can be expected whilst if within a wavelength of a corner the increase will be about 12 dB. For points which are at least a wavelength away from a boundary the variation will however be small and can be ignored. For the transfer mobility, the effect upon the mean level of the distance between the two points can be ignored if the points are less than a wavelength apart. Under such conditions Y^{tr}/Y^{pt} will therefore equal unity. Although where the points are greater than a wavelength apart, the mean of the transfer mobility magnitude can be expected to be lower than that of the characteristic mobility, the details are dependent upon the distance involved. Under such circumstances it is difficult to deduce a relationship for the mean of Y^{tr}/Y^{pt}.

For a point mobility the envelope which bounds the peaks and troughs is equally positioned above and below the mean value by the factor

$$\beta_{\max} = 2\epsilon_v/\pi\eta\omega_v. \tag{19}$$

Combining equations (17) and (19), one finds that the envelope defining the maximum variation of the point mobility in the resonance region is, for positions away from the edge, given by

$$Y^{pt}|_{\max} = Y_\infty + 7{\cdot}2c_L h/\pi A\eta\omega_v \tag{20}$$

and the minimum by

$$Y^{pt}|_{\min} = Y_\infty - 7{\cdot}2c_L h/\pi A\eta\omega_v. \tag{21}$$

Since for a transfer mobility the response point can be positioned at a node, the lower bound of the envelope, other than zero, cannot be defined. The maximum of the envelope will however be likewise that for the point mobility. Thus whilst the lower limit of the magnitude of Y^{tr}/Y^{pt} cannot be defined, the upper limit for the magnitude of Y^{tr}/Y^{pt} can be given by

$$Y^{tr}/Y^{pt}|_{\max} = (Y_\infty \pi A \eta \omega_v + 7{\cdot}2 c_L h)/(Y_\infty \pi A \eta \omega_v - 7{\cdot}2 c_L h). \tag{22}$$

As regards the phase in the resonance region, the wavefield is so complex that such relationships between that of the point and transfer mobilities cannot be determined.

2.4. MEASUREMENTS

To support the theoretical study a number of experimental mobility measurements have been undertaken. The purpose of the measurements was to validate that a point mobility will exhibit all of the mass, stiffness and resonance regions and that for each region different relationships between the point and transfer mobility can be expected and to a certain extent predicted. Because the framework of the approach has as its reference the general form of the point mobility, machine details, other than the mount-plate type, add little to the results. For interest, therefore, as the basis for the measurements three medium sized fan units from air conditioning systems were used.

The first fan unit had a base consisting of three flanges welded to the machine's main body; see Figure 16 for a schematic diagram. Theory suggests that for a transfer mobility along a flange the magnitude will, in the stiffness controlled region, be approximately a decade below that of the point mobility. In the mass controlled region Y^{tr}/Y^{pt} can be expected to be constant whilst in the resonance region the relationship will be variable. A typical point and transfer mobility shown in Figure 17 confirms these expectations; the stiffness region extends over the frequency range 80–800 Hz and the transfer mobility over much of this range, i.e., 300 Hz to 800 kHz, is a decade or more below the point mobility.

The base of the second fan unit was formed from a single plate with the mount points upon bent-in flanges (see Figure 18) so that the structure of the flange was not as defined as for the first unit. It is suggested that the bent-in flange can be

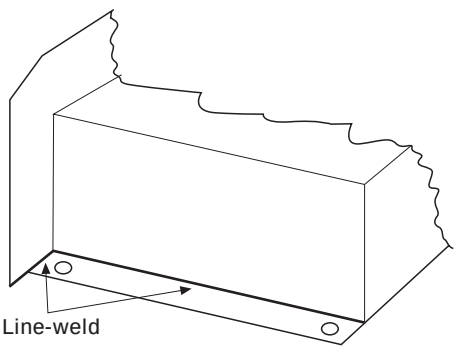

Figure 16. For fan 1 flange is welded along two sides.

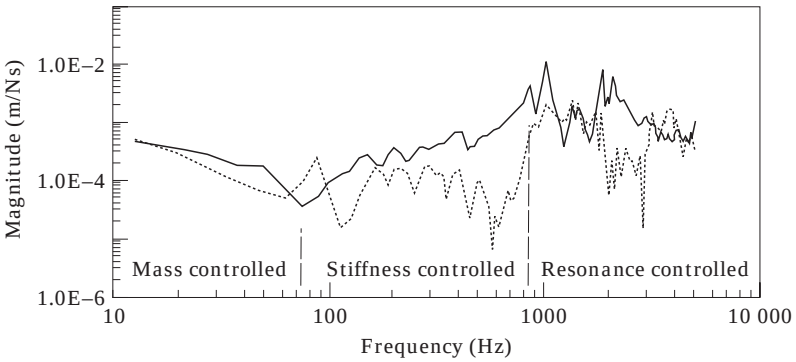

Figure 17. Point and transfer mobility for fan 1. —, Y^{11}; . . . . , Y^{12}.

thought of as a hybrid between a flange- and a plate-like base. Though the frequency resolution is poor and accuracy limited it is suggested that for frequencies below 70 Hz the point mobility is (see Figure 19) mass controlled. Between 70 Hz and 100 Hz the slope of the point mobility is however steeper than expected for a stiffness controlled region whereupon the region is probably

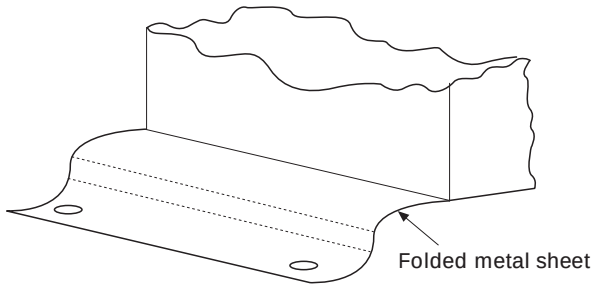

Figure 18. For fan 2 flange is formed from a bend in metal sheet.

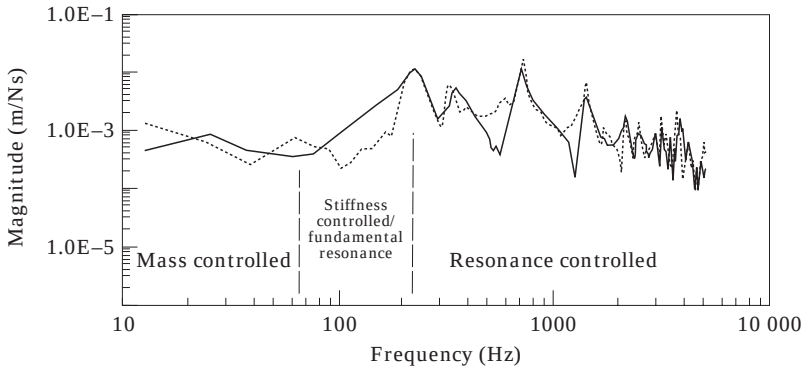

Figure 19. Point and transfer mobility for fan 2. Key as Figure 17.

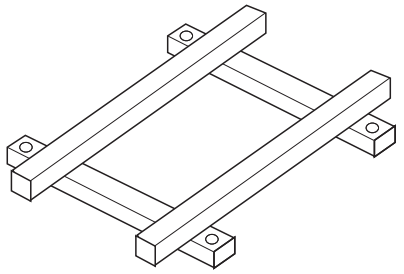

Figure 20. The base of fan 3 is formed from a series of connected beams.

dominated by the fundamental resonance. That the transfer mobility magnitude in the region is significantly less than that of the point mobility is, it is suggested, indicative of uncoupling via the twisting action identified in Figure 9.

For the third fan, the base was constructed from a series of connected beams (see Figure 20). The mount condition is therefore neither plate- or flange-like and hence a long stiffness controlled region cannot be expected. Instead the mass controlled region will be directly followed by a resonance region and, due the beams acting as waveguides, the point and transfer mobilities can, for all frequencies, be expected to have similar trends; see Figure 21.

3. FLOOR MOBILITIES

In order to formulate both the source descriptors and coupling functions of a system the effective mobilities of both source and receiver have to be assembled. As well as for machines, relationships between the mobilities of the recipient structure do therefore also have to be considered.

So to be apt for building engineering applications, the recipient is designated to be a floor within a building. Since a floor is not a free body, a mass controlled region will not be seen in the point mobility. As regards the general form of the receiver mobility, the lower frequency asymptote will therefore be a stiffness controlled region. For frequencies above the floor's fundamental resonance, i.e.,

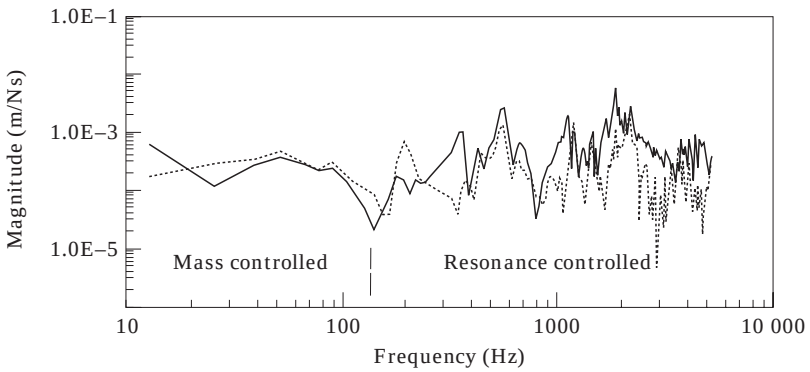

Figure 21. Point and transfer mobility for fan 3. Key as Figure 17

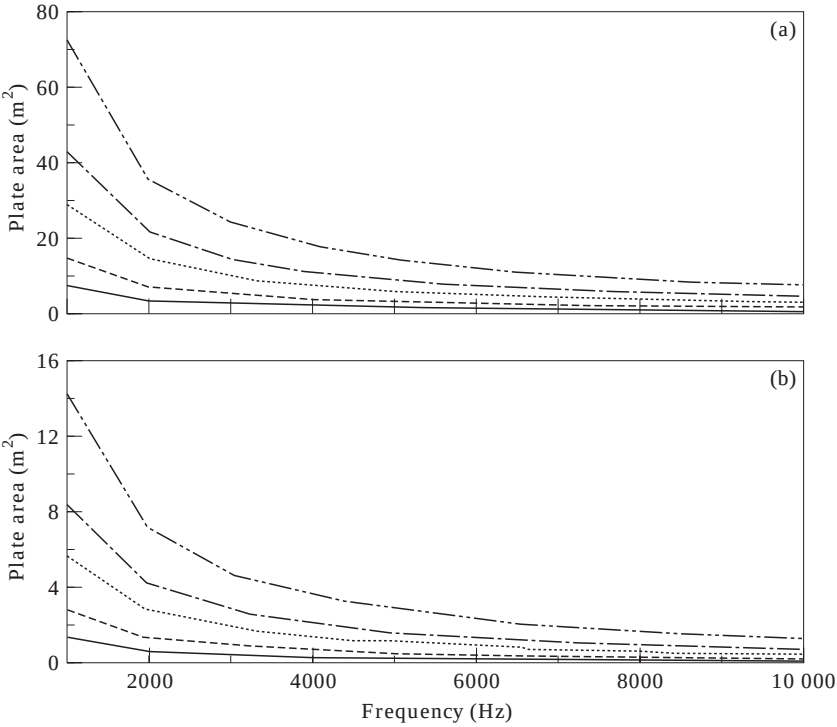

Figure 22. For concrete and $\eta = 0{\cdot}01$, area of plate needed for Skudrzyk's high frequency limit (a) and lower frequency limit (b). —, $h = 50$ mm; - - - , $h = 100$ mm; . . . . , $h = 200$ mm; — · — · —, $h = 300$ mm; — · · —, $h = 500$ mm.

the resonance region, it is interesting to consider the frequency dependence of the floor area and thickness required for α to equal unity (Skudrzyk's high frequency region) and for α to equal five (the low frequency limit). Hence, upon assuming material properties of concrete and a loss factor of 0·01, the plate area required for $\alpha = 1$ is shown in Figure 22(a), and for $\alpha = 5$ in Figure 22(b). From Figure 22(a), it is suggested that the ranges of plate areas exhibited are comparable to those found in typical building engineering installations. Indeed, even for the extreme case shown of a 500 mm thick concrete floor and excitation frequency of 1 kHz, the area required for $\alpha = 1$ is only 72 m^2. For the floor mobilities, it is suggested too therefore that is it likely that Skudrzyk's very high frequency limit will also be reached: i.e., $\alpha < 1$. For this region, reflections from the boundaries do not contribute to the plate response whereby the finite nature of the floor can be ignored and an infinite structure assumed. As regards the general form of the recipient mobility the upper asymptote is therefore an infinite region; see Figure 23. This in agreement with measurements by Fahy [11].

Appreciating that a floor is plate-like means that the above work concerning a machine mount with a plate-like base is also applicable to the floor. Hence for a floor in a stiffness controlled region, it is known that if the points are close to each other and are away from constraining edges, Y^{tr} and Y^{pt} will be approximately equal. Where one point is close to an edge or both points are separated by large

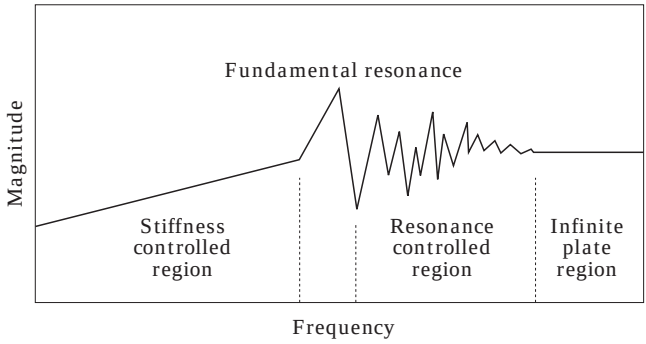

Figure 23. Generalized point mobility of floor mount.

distance then discrepancies between the mobilities will however occur. Likewise, for the resonance region of the floor point mobility, application of the plate-like work of the machine mount suggests that for frequencies above the fundamental plate resonance, Y^{tr}/Y^{pt} relationships are difficult to establish and best considered statistically.

For the infinite region of the floor mobility Y^{tr}/Y^{pt} can however be expected to be a smooth function. In polar co-ordinates the ratio can be written as

$$Y^{tr}/Y^{pt} = \mathrm{H}_0^{(2)}(kr) - \mathrm{H}_0^{(2)}(-\mathrm{i}kr) \tag{23}$$

where $\mathrm{H}_0^{(2)}$ is a Hankel function of the second order with r the distance between the two points.

By plotting the magnitude of Y^{tr}/Y^{pt} versus kr, see Figure 24, it is seen that for kr greater than 2·5 the point mobility magnitude is at least twice that of the transfer mobility. Since the decrease seen is due to divergence the phase of Y^{tr}/Y^{pt} can similarly be expected to decrease with kr.

Where two points are greater than an eighth of a wavelength apart asymptotic values of the Hankel function can be used such that

$$\mathrm{Y}(0, r) = \mathrm{Y}_\infty(2/2kr)^{1/2}\,\mathrm{e}^{-\mathrm{i}k(r-\gamma/8)}, \tag{24}$$

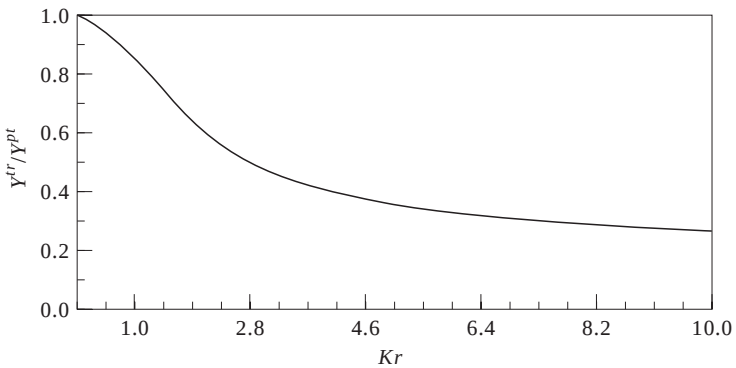

Figure 24. Y^{tr}/Y^{pt} upon an infinite plate.

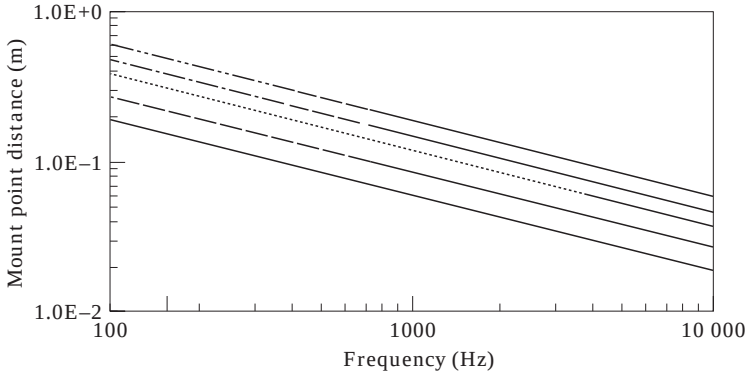

Figure 25. Maximum distance for $Y^{tr}/Y^{pt} \approx 1$ upon a concrete floor. Key as Figure 22.

whilst if r is small, power developments can be used to give the simple result that providing the distance involved is less than an eighth of a wavelength the transfer mobility will approximate to the point mobility; $Y^{tr}/Y^{pt} = 1$. In Figure 25 the frequency limit of this criteria is plotted for different thicknesses of concrete.

4. MACHINE FREE VELOCITIES

With respect to the source descriptor and coupling function formulation the final components which need to be considered are the free velocities of the machine. The free velocity of a machine mount point being that velocity manifested when the machine is run under normal operating conditions but without connection to any external structure. Likewise the mobilities, relationships between the free velocities are considered.

The free velocity is a function of all of the machines internal mechanisms. To be obtained via a theoretical model that model would therefore have to include all of the machine components including both passive and active subsystems i.e., excitation and transmission elements. Clearly the difficulties involved with obtaining data for all components and theoretically connecting all together are intractable. More importantly however the excitation mechanisms of machines are so varied that, unlike structural characteristics where for example a mount point can be modelled as a plate attached to a mass, a general model cannot be considered for free velocities. A theoretical analysis of free velocities is therefore difficult to conceive. Hence, the study instead is concentrated upon measured data. To be consistent with the analysis of the mobilities relationships between free velocities are considered for each of the mass, stiffness and resonant regions.

4.1. MASS CONTROLLED REGION

In the mass controlled region the machine moves as a rigid body. Where there is a single internal excitation source, or else all the internal excitations are coherent, the phase difference between the free velocities will be discretized at

either $\pm\pi$ or 0. For a rotational mode about the x-axis the relationships will be

$$\theta\{V_{sf}^1\} - \theta\{V_{sf}^2\} = 0, \qquad \theta\{V_{sf}^1\} - \theta\{V_{sf}^3\} = \pm\pi, \qquad \theta\{V_{sf}^1\} - \theta\{V_{sf}^4\} = \pm\pi, \tag{25a–c}$$

whilst for a translational mode all the free velocities will be in phase.

With respect to magnitude relationships, nothing can be reasoned unless assumptions for the excitation mechanism, the structure of the machine and the positions of the mount points are introduced. As for the mobility relationships it is suggested therefore that for reasons of stability the mount points of the machine are positioned symmetrically around the machines centre of gravity. Providing the internal excitations have similar symmetrical properties, it can then be deduced that all the free velocities in the mass controlled region will be of approximately equal magnitude.

4.2. STIFFNESS CONTROLLED REGION

In the stiffness controlled region the machine no longer moves as a rigid body and the magnitudes and phases of the free velocities depend upon the details of the machine. With respect to magnitude and phase relationships nothing can therefore be stated other than that under the symmetrical properties outlined above it is possible that the magnitude of all the free velocities will exhibit similar trends.

4.3. RESONANCE CONTROLLED REGION

The wave behaviour in the resonance region dictates that again magnitude and phase relationships cannot be determined. The possible exception is that for approximately symmetrical conditions of both structure and excitation mechanism the magnitudes of the free velocities will all exhibit a similar trend.

4.4. MEASUREMENTS

Free velocity measurements were taken of the three fan units considered in the analysis of the mobilities. To approximate the free condition the units were suspended by low resilience restraints [12].

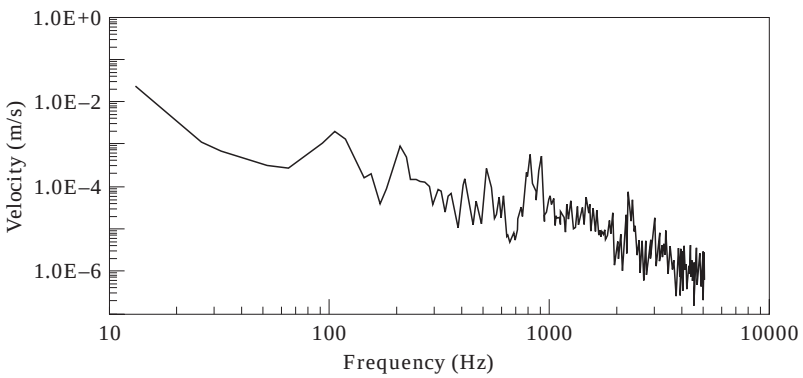

Figure 26. Free velocity for fan 1.

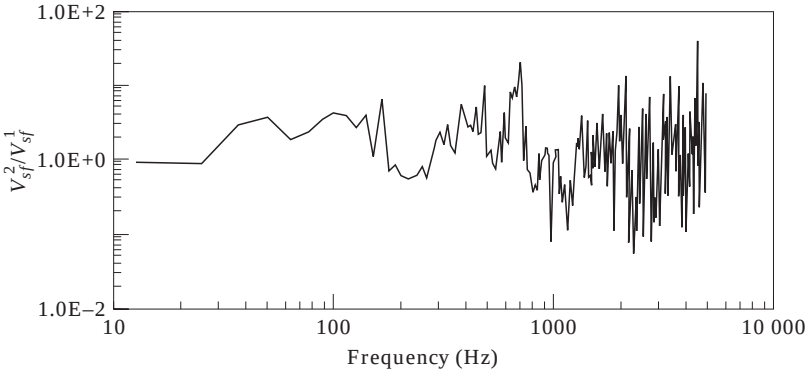

Figure 27. Ratio of two free velocities for fan 1.

For the first fan unit the magnitude of a typical free velocity is shown in Figure 26. The spectrum has a decreasing trend with frequency indicating that the majority of the activity is contained in the low frequencies. The magnitude ratio of the free velocities at two points is shown in Figure 27. In the mass controlled region, (below 80 Hz), the free velocities are within 10 dB suggesting approximate symmetrical properties. For both the stiffness and resonant controlled regions the free velocities also have similar trends. The variations have however increased to about ± 20 dB.

The ratio of two typical free velocities of the second fan unit is shown in Figure 28. A similarity trend is again observed but the variations are within a range of about 30 dB. This is especially noticeable in the mass controlled region.

Results for the third fan are shown in Figure 29. The free velocities again follow a similar trend where the range of variation is 10 dB.

5. CONCLUDING REMARKS

Work towards understanding the components involved in the source descriptor and coupling function formulation has been undertaken. Hence for both machines

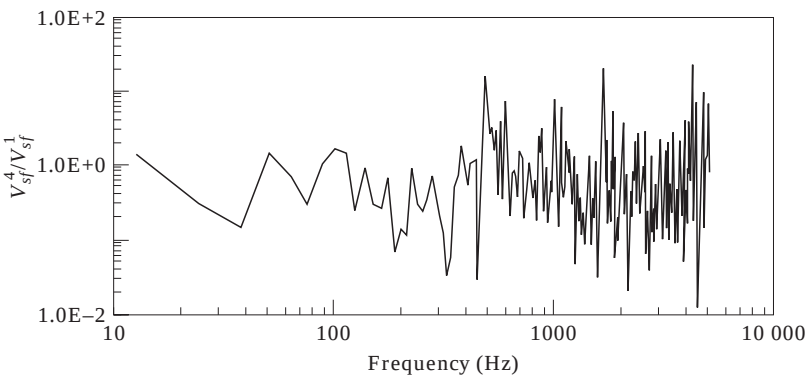

Figure 28. Ratio of two free velocities for fan 2.

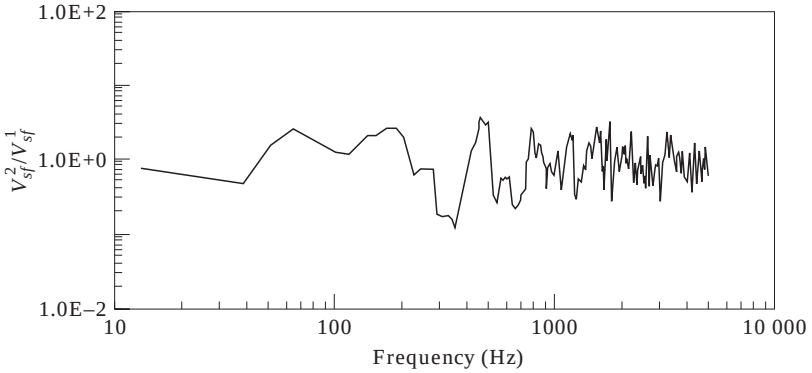

Figure 29. Ratio of two free velocities for fan 3.

and floors relationships between point and transfer mobilities have been considered and free velocity relationships for machines also studied.

The point mobility of a typical machine mount can be generalized as operating in either a mass, stiffness or resonance controlled region. For the floor the mass controlled region can be disregarded but at high frequencies, an additional infinite region also needs to be considered.

Where the source is mass controlled Y^{tr}/Y^{pt} depends upon the inertial properties and position of mount points. If symmetry is assumed, the magnitude of Y^{tr}/Y^{pt} will be either unity or paired in accordance with equation (8) whilst the phase will be discretized at either 0 of $\pm\pi$, (see equations (9) and (10)).

For the stiffness control region Y^{tr}/Y^{pt} for the machine depends upon whether the mount is plate- of flange-like. For a plate-like footing Y^{tr}/Y^{pt} is again either unity or, upon assuming symmetry, paired in accordance with equation (8). The distinguishing factor is the relative position of the points to the plate edges. For two mount points upon a flange-like footing the transfer mobility in the stiffness region is a decade below the point mobility. Effectively the two points are therefore uncoupled and the transfer terms in the mobility matrix can be ignored. Where the floor is modelled as a plate relationships between the point and transfer mobilities are as for the plate-like footing. The phase of both point and transfer mobilities in a stiffness region is always $\pi/2$.

For the resonance controlled region relationships for Y^{tr}/Y^{pt} are difficult to establish for both machine or floor unless considered as a statistical distribution. In the infinite region, expected for a floor at high frequencies, Y^{tr}/Y^{pt} can however (providing two points are greater than an eighth of a wavelength apart) be determined by using equation (24).

For free velocity the complexity and variability of machine construction and operation is such that the only deterministic relationship deduced is that, providing the machines internal excitation mechanisms are all coherent, the phase in the mass controlled region will be descretized at 0 or $\pm\pi$. Based upon measurements of three machines, it is also tentatively suggested that providing both the structure and excitation mechanisms have approximate symmetrical spatial properties then

the magnitudes of free velocities at different mount points will follow a similar trend.

In summary, relationships between point and transfer mobilities and amongst free velocities have been studied. By using these relationships, source characterization for multi-point systems can now be undertaken without restriction to specific machines and structures. Work by Fulford [13] with respect to this is to be reported in a later paper.

ACKNOWLEDGMENT

This study was financially supported by the Engineering and Physical Sciences Research Council, U.K. The support is gratefully acknowledged.

REFERENCES

1. J. M. Mondot and B. A. T. Petersson 1987 *Journal of Sound and Vibration* **114**, 507–518. Characterization of structure-borne sound sources: the source descriptor and coupling function.
2. R. A. Fulford and B. M. Gibbs 1996 *Journal of Sound and Vibration* **204**, 659–677. Structure-borne sound power and source characterization in multi-point connected systems. Part 1: Initial Study.
3. B. A. T. Petersson and J. Plunt 1980 *Chalmers University of Technology*, *Sweden*, *Department of Building Acoustics*, *Report* 80–19. Structure-borne sound transmission from machinery to foundations.
4. M. S. Kompella and R. J. Bernhard 1993 *Proceedings of SAE Noise and Vibration Conference*, *Society of Automotive Engineers*. Measurement of the statistical variations of structural–acoustic characterizations of automotive vehicles.
5. B. A. T. Petersson and J. Plunt 1980 *Chalmers University of Technology*, *Sweden*, *Department of Building Acoustics*, *Report* 80–19. Structure-borne sound transmission from machinery to foundations.
6. R. Szilard 1974 *Theory and Analysis of Plates. Classical and Numerical Methods*. Englewood Cliffs, New York: Prentice-Hall.
7. G. B. Warburton 1979 *Earthquake Engineering and Structural Dynamics* **7**, 327–334. Response using the Rayleigh–Ritz method.
8. B. M. Gibbs and Y. Shen 1987 *Journal of Sound and Vibration* **112**, 469–485. The predicted and measured bending vibration of an L-combination of rectangular thin plates.
9. E. Skudrzyk 1980 *Journal of the Acoustical Society of America* **67**, 1105–1135. The mean-value method of predicting the dynamic response of complex vibrators.
10. L. Cremer, M. Heckl and E. Ungar 1973 *Structure-borne sound*. Berlin; Springer-Verlag pp 331–332. Second edition.
11. F. J. Fahy and M. E. Westcott 1978 *Journal of Sound and Vibration* **57**, 101–129. Measurement of floor mobility at low frequencies in some buildings with long floor spans.
12. International Standards Organization 1993 *ISO/DIS* 9611.2. Acoustics–Characterisation of sources of structure-borne sound with respect to the air-borne sound radiation of connected structures–measurement of velocity at the contact points of machinery when resiliently mounted.
13. R. A. Fulford 1995 *University of Liverpool*, *Ph.D. Thesis*. Structure-borne sound power and source characterisation in multi-point-connected systems.